

Scientific Hypothesis Generation by Large Language Models: Laboratory Validation in Breast Cancer Treatment

Abbi Abdel-Rehim¹, Hector Zenil^{2,3}, Oghenejokpeme Orhobor⁴, Marie Fisher⁵, Ross J. Collins⁵, Elizabeth Bourne⁵, Gareth W. Fearnley⁵, Emma Tate⁵, Holly X. Smith⁵, Larisa N. Soldatova⁶, Ross D. King^{1,7}

¹Department of Chemical Engineering and Biotechnology, University of Cambridge, CB3 0AS, U.K.

²School of Biomedical Engineering and Imaging Sciences, King's College London, SE1 7EU, U.K.

³The Alan Turing Institute, British Library, London, NW1 2DB, U.K.

⁴The National Institute of Agricultural Botany, Cambridge, CB3 0LE, U.K.

⁵Arctoris Ltd, Oxford, OX14 4SA, UK.

⁶Department of Computing, Goldsmiths, University of London, SE14 6NW, U.K.

⁷Department of Computer Science and Engineering, Chalmers University, S-412 96 Göteborg, Sweden.

Abstract

Large language models (LLMs) have transformed AI and achieved breakthrough performance on a wide range of tasks that require human intelligence. In science the most interesting application of LLMs is for hypothesis formation. A feature of LLMs, which results from their probabilistic structure, is that the output text is not necessarily a valid inference from the training text. These are termed "hallucinations", and are harmful in many applications¹. In science some hallucinations may be useful: novel hypotheses whose validity may be tested by laboratory experiments². Here, we experimentally test the application of LLMs as a source of scientific hypotheses using the domain of breast cancer treatment. We applied the LLM GPT4 to hypothesize novel synergistic pairs of FDA-approved non-cancer drugs that target the MCF7 breast cancer cell line relative to the non-tumorigenic breast cell line MCF10A. In the first round of laboratory experiments GPT4 succeeded in discovering three drug combinations (out of twelve tested) with synergy scores above the positive controls. GPT4 was then asked to generate new combinations based on its initial results, this resulted in the discovery of three more combinations with positive synergy scores (out of four tested). A limitation of GPT4 as a generator of hypotheses was that its explanations were formulaic and unconvincing, suggesting GPT4 knew more than it could explain. We conclude that LLMs are a valuable source of scientific hypotheses.

Main

The world has been stunned by the success of Large Language Models (LLMs). They have achieved breakthrough performance on a wide range of conversation-based tasks that previously required human intelligence. The overall architecture of LLMs is remarkably simple: they map input token strings to output token strings using deep neural networks (DNNs). Their power comes from being trained on very large general corpuses (substantial percentages of the whole text-based internet), and the use of very large numbers of both tokens ($> 10^4$) and parameters ($> 10^{12}$). The success of LLMs is surprising given that they don't use any explicit model of the world, nor explicit internal symbols, nor do they have any physical grounding in the world. All of these were assumed by most AI scientists to be essential for such intelligent behaviour.

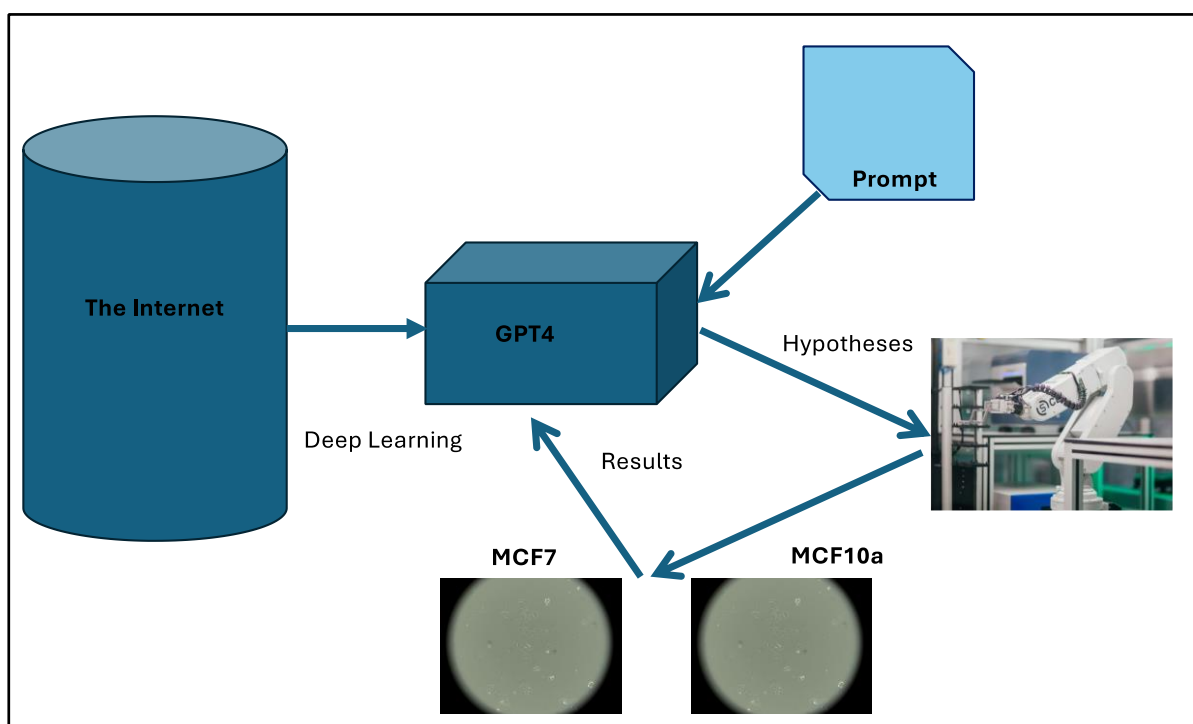


Figure 1. The overall structure of our experiments. GPT4 was previously trained on data on a large fraction of the text on the internet. We engineered prompts to request from GPT4 synergistic pairs of drugs that are toxic to the breast cancer cell line MCF7, but not to the non-cancer breast cell line MCF10a. These are the hypotheses that we experimentally tested using laboratory automation.

LLMs can be applied to many aspects of science: to summarize texts^{3,4}, to analyze data⁵, to write papers and code⁶, to formalize knowledge⁷, to answer questions⁸, etc. However, the most exciting application for LLMs in science is for generating novel hypotheses. Despite the clear potential of LLMs for hypothesis generation their utility for hypothesis generation has been little investigated.

The architecture of LLMs entails that the output string is the most likely one given the input string and the training data. For science these strings may be interpreted as scientific hypotheses. Due to their internal complexity and sophistication LLMs have the potential to go beyond existing text-based scientific hypothesis generation tools^{9,10}. The generation of hypotheses by LLMs is closely related to the phenomena of "hallucinations". These are LLM outputs that are not valid inferences from the training data. Some hallucinations may be simply factually wrong. For others, their validity is uncertain. Hallucinations are a serious problem in many applications. For example, in science it is not

acceptable to hallucinate (make up) false references. However in scientific hypothesis generation hallucinations may be useful: probable novel hypotheses whose validity may be objectively tested by laboratory experiments.

Here we use laboratory experiments to test the utility of the general purpose LLM GPT4 for scientific hypothesis generation (Figure 1). We employed breast cancer as the test domain. In our experiments breast cancer cells were exemplified by MCF7 (an epithelial breast cancer cell line); non-tumorigenic breast cells were exemplified by the epithelial cell line MCF10A. We provided GPT4 with a prompt that had several aims: 1) Identify novel drug combinations that would have a significant impact on MCF7 cell lines; 2) Avoid harming MCF10A the control cell line; and 3) Design combinations that were possibly synergistic. We also had additional requirements related to the drugs themselves: at least one of the drugs in every pair should not be an anti-neoplastic drug, and that the drugs should be affordable, accessible, and preferably FDA-approved. All the prompts used are given in figure S1. The list of recommendations are in Table 1a (complete hypotheses in Figure S1). Interestingly, all the drug combinations hypothesized were exclusively non-cancer drugs (suggesting a possible limitation in GPT4 understanding of its instructions). The combinations were however novel, and we could not find any of them reported for breast cancer in the literature. We did find that a number of the drugs had been investigated in the cancer literature, and that several of the drugs had been tested against MCF7 (Supplementary materials Appendix B).

In addition to hypothesizing drug combination we prompted GPT4 to provide two positive controls that are commonly used against breast cancer in clinic, and likely have an impact on MCF7; as well as two negative control combinations that would be unlikely to cause harm to MCF7 (Figure S2, S3). It may have been wiser to select the controls ourselves. But we judged that GPT4 did a fair job in its selections (Table 1b).

	Drug1	Drug2
1	Disulfiram (Alcoholism)	Simvastatin (Hypercholesterolemia)
	"Disruption of lipid rafts by simvastatin may enhance disulfiram-induced oxidative stress, leading to apoptosis in MCF7 cells."	
2	Celecoxib (Pain/Inflammation)	Quinacrine (Malaria/Anti-inflammatory)
	"Reduced inflammatory signaling by celecoxib may enhance quinacrine-induced impairment of autophagy, leading to apoptosis in MCF7 cells."	
3	Acarbose (Diabetes)	Itraconazole (Fungal Infections)
	"Acarbose-induced glucose deprivation may enhance the effect of itraconazole on disrupting cell membrane integrity, leading to apoptosis in MCF7 cells."	
4	Dipyridamole (Blood Thinner)	Mebendazole (Parasitic Infections)
	"Dipyridamole-induced increase in cAMP levels may enhance the effect of mebendazole on cell cycle arrest, leading to apoptosis in MCF7 cells."	
5	Atorvastatin (Hypercholesterolemia)	Metronidazole (Bacterial Infections)
	"Atorvastatin-induced disruption of lipid rafts may enhance the effect of metronidazole-induced DNA damage, leading to apoptosis in MCF7 cells."	
6	Allopurinol (Gout)	Chloroquine (Malaria)
	"Allopurinol-induced reduction of uric acid may enhance the effect of chloroquine-induced impairment of autophagy, leading to apoptosis in MCF7."	
7	Cimetidine (Gastric Acid Reducer)	Disulfiram (Alcoholism)

	"Cimetidine-induced reduction of gastric acid may enhance the effect of disulfiram-induced oxidative stress and DNA damage in MCF7 cells."	
8	Memantine (Alzheimer's)	Niclosamide (Parasitic Infections)
	"Memantine-induced reduction of glutamate excitotoxicity may enhance the effect of niclosamide-induced energy depletion, leading to cell death in MCF7 cells."	
9	Furosemide (Diuretic)	Mebendazole (Parasitic Infections)
	"Furosemide-induced reduction of sodium reabsorption may enhance the effect of mebendazole on cell cycle arrest, leading to apoptosis in MCF7 cells."	
10	Sildenafil (Erectile Dysfunction)	Disulfiram (Alcoholism)
	"Sildenafil-induced increase in cGMP levels may enhance the effect of disulfiram-induced oxidative stress and DNA damage in MCF7 cells."	
11	Itraconazole (Fungal Infections)	Atenolol (Hypertension)
	"Atenolol-induced reduction of stress signaling may enhance the effect of itraconazole on disrupting cell membrane integrity, leading to apoptosis in MCF7 cells."	
12	Hydroxychloroquine (Malaria, Rheumatoid Arthritis)	Disulfiram (Alcoholism)
	"Hydroxychloroquine-induced impairment of autophagy may enhance the effect of disulfiram-induced oxidative stress and DNA damage in MCF7 cells."	

Table 1a. GPT4 generated drug combination hypotheses.

	Drug1	Drug2
1	Doxorubicin	Cyclophosphamide
	<p>Positive Control.</p> <p>Combination FDA approved to treat Breast Cancer</p> <p>Doxorubicin is an anthracycline that intercalates into DNA and inhibits topoisomerase II, causing DNA damage. Cyclophosphamide is an alkylating agent that causes DNA damage.</p> <p>"The combination targets DNA integrity through multiple mechanisms, which may be effective in MCF7 cells with high proliferative capacity."</p>	
2	Fulvestrant	Palbociclib
	<p>Positive Control.</p> <p>Individually FDA approved to treat Breast Cancer</p> <p>Fulvestrant is a selective estrogen receptor degrader (SERD) that blocks and degrades estrogen receptors. Palbociclib is a CDK4/6 inhibitor that blocks cell cycle progression.</p> <p>"The combination targets both estrogen signaling and cell cycle progression, which may be effective in estrogen receptor-positive MCF7 cells."</p>	
3	Allopurinol (Xanthine Oxidase Inhibitor)	Omeprazole (Proton Pump Inhibitor)

	Negative Control "Allopurinol is used to treat gout and hyperuricemia, and omeprazole is used to reduce stomach acid. Neither drug targets pathways relevant to MCF7 breast cancer cell growth or survival, and they are not expected to have an effect on MCF7 cells."	
4	Diphenhydramine (Antihistamine)	Omeprazole (Proton Pump Inhibitor)
	Negative Control "Diphenhydramine and cetirizine are antihistamines used to treat allergy symptoms. Neither drug targets pathways relevant to MCF7 breast cancer cell growth or survival, and they are not expected to have an effect on MCF7 cells."	

Table 1b. GPT4 generated positive and negative control combinations.

Results

Using the method described below we screened the twelve pairs of compounds proposed by GPT4 (Table 1a). We investigated two properties of the pairs: 1) The specificity of the combination for MCF7 v MCF10A, and 2) The additivity/synergy of the combination. (Additivity occurs when the combination of the effects of two drugs is not less than either of the two drugs acting independently. Synergy describes the situation when the effect of the combination is greater than that of the most effective drug (highest single agent)). To determine drug additivities/synergies we employed SynergyFinder 3.0 to calculate HSA (highest single agent) synergy scores for all combinations (Table 2). There were six additive interactions combinations with positive synergy scores for MCF7: itraconazole + atenolol, simvastatin + disulfiram, dipyridamole + mebendazole, furosemide + mebendazole, disulfiram + hydroxychloroquine, and the positive control doxorubicin + cyclophosphamide. The initial three hypothesised combinations resulted in HSA scores surpassing those of the positive controls. Synergistic areas were found within the drug response matrices belonging to ten out of twelve of the hypothesized drug combinations (Table S2). We found that eight out of the twelve hypothesized combinations resulted in a higher HSA score in varying degrees for MCF7 compared to MCF10A (Table 2, cf. Table 2 and Table S3). In Table S12 we summarize the literature on the hypotheses proposed by GPT4 and the anti-cancer properties of the drugs selected. We found underlying support in literature for three out of the latter screened six combinations with positive synergy scores, while the remaining three remain unclear.

Drug 1	Drug 2	HSA score (MCF7)	Specificity (MCF7)
Itraconazole	Atenolol	4.83	7.03
Simvastatin	Disulfiram	3.29	1.85
Dipyridamole	Mebendazole	2.49	3.69
Doxorubicin*	Cyclophosphamide*	1.02	3.27
Furosemide	Mebendazole	0.72	6.14
Disulfiram	Hydroxychloroquine	0.60	3.51
Acarbose	Itraconazole	-1.36	-1.33
Disulfiram	Sildenafil	-1.63	0.85
Allopurinol	Chloroquine	-1.87	2.24

Celecoxib	Quinacrine	-2.21	-3.27
Fulvestrant*	Palbociclib*	-2.59	-0.49
Memantine	Niclosamide	-2.61	-2.23
Disulfiram	Cimetidine	-3.06	-8.17
Allopurinol**	Omeprazole**	-3.85	-6.2
Atrovastatin	Metronidazole	-4.84	-6.3
Diphenhydramine**	Cetirizine**	-9.25	-6.28

Table 2. HSA synergy score for each combination. “Specificity” indicates synergy score differences between the cell lines ($HSA_{MCF7} - HSA_{MCF10A}$). *Positive controls, **negative controls. Combinations selected for further validation are marked in bold. The combinations in blue have positive synergy scores .

To better understand the utility of the paired compounds we tested the individual drugs (Table 3). From the drugs in the positive controls pairs only doxorubicin was found to result in an IC50 value below the maximum dose of 25uM in both cell lines. For MCF7 there were five additional drugs that resulted in IC50 values below the same threshold, with Disulfiram and Niclosamide showing comparatively high toxicity (Table 3). Several more drugs were toxic to the cell lines, but failed to reduce the viability to such an extent where an IC50 value could be derived (Table S4 and S5). In total, twelve out of the eighteen non-control drugs showed toxicity towards MCF7: celecoxib, chloroquine, dipyridamole, disulfiram, hydroxychloroquine, itraconazole, mebendazole, niclosamide, quinacrine, sildenafil and simvastatin. Out of these drugs, dipyridamole, disulfiram, mebendazole and quinacrine showed high specificity towards MCF7 (cf. Table S4 and S5). While many of these drugs had been studied in cancer cell lines, they are not cancer drugs. Fulvestrant, a positive control cancer drug also showed preference for MCF7.

Eleven out of eighteen compounds reduced viability of the control cell line MCF10A. When excluding the highest concentration of 25 uM, these numbers change to 6/18 and 8/18 compounds for MCF7 and MCF10A respectively. The ten drugs that showed highest toxicity towards MCF7 were re-screened to achieve sufficient replicates (n=3) in order to validate their toxicity.

In an additional experiment, twelve drugs were retested from the first round (n >=3 replicates). An ANOVA two-way test with three replicates was used to calculate significance of changes to viability compared to the internal control drug Allopurinol for both cell lines (S6, S7). Two of the retested drugs were initially used as positive controls for MCF7 (doxorubicin and fulvestrant). Out of twelve retested drugs, dipyridamole, disulfiram, niclosamide and quinacrine significantly reduced the viability of MCF7 when considering concentrations up to 3.84 μ M. The two positive control drugs doxorubicin and fulvestrant also targeted MCF7. When considering all concentrations (including 25 μ M which is quite high), all but hydroxychloroquine results in a significant impact on MCF7. Despite this, the toxicity of hydroxychloroquine at 25 uM is persistent and substantial. IC50 values could only be calculated for 5/11 compounds (Table S8), disulfiram and doxorubicin showing sub micromolar IC50 values of 0.059 and 0.3 μ M respectively. This was followed by niclosamide at 1.22 μ M, quinacrine at 4.71 μ M and chloroquine at 10.62 μ M. However, the remaining compounds were still toxic to MCF7 (Table S9). Calculated IC50, and viability values for MCF10A can be found in Tables S8 and S10.

Drug	MCF7 IC50 (uM)	MCF7 p-val	MCF10A IC50 (uM)	MCF10A p-val
Allopurinol**	>25	-----	>25	-----
Atenolol	>25	0.003	>25	0.118
Celecoxib	5.325	0.046	22.573	0.185
Disulfiram	0.204	0.008	>25	0.095
Fulvestrant*	>25	0.020	>25	0.430
Itraconazole	>25	0.021	>25	0.077
Sildenafil	>25	0.011	>25	0.212
Cimetidine	>25	0.012	>25	0.023
Mebendazole	>25	0.025	15	0.018
Metronidazole	>25	0.039	>25	0.031
Atorvastatin	>25	0.131	3.795	0.009
Chloroquine	>25	0.202	>25	0.030
Doxorubicin*	0.303	0.054	0.435	0.034
Memantine	>25	0.834	>25	0.022
Niclosamide	0.699	0.066	0.061	0.021
Acarbose	>25	0.251	>25	0.019
Cetirizine**	>25	0.210	>25	0.257
Cyclophosphamide*	>25	0.276	>25	0.499
Diphenhydramine**	>25	0.684	>25	0.500
Dipyridamole	>25	0.056	>25	0.093
Furosemide	>25	0.246	>25	0.188
Hydroxychloroquine	>25	0.118	>25	0.944
Omeprazole**	>25	0.082	>25	0.245
Palbociclib*	>25	0.414	>25	0.650
Quinacrine	3.848	0.082	10.183	0.116
Simvastatin	5.634	0.106	7.17	0.120

Table 3. Single drug treatments. For either cell line, the IC50 values were calculated and declared (n=1). Significance (p-value) of changes evoked by drug treatments when compared to positive control (Allopurinol) are also reported. ANOVA two-way significance is used for the samples, most of which are single replicates. P-values are declared for both cell lines. *=Positive controls, ** = negative controls. Numbers in bold significant <0.05. Blue significant against MCF7. Red significant against MCF10A. Green significant against MCF7 and MCF10A

After the results from the first round of experiments were complete we investigated whether GPT4 could improve its hypotheses through use on the results from its initial hypotheses. We provided GPT4 with a summary of the results from the primary screen (Figure S4), and prompted GPT4 to consider combinations containing drugs from the positive controls as well. GPT4 hypothesized four combinations based on this information: disulfiram + fulvestrant, disulfiram + mebendazole, mebendazole + quinacrine, and disulfiram + quinacrine (Table 4). In addition we re-tested three combinations that resulted in positive synergy scores from the primary screening achieving more robust results, these combinations were disulfiram + simvastatin, disulfiram + hydroxychloroquine,

and dipyridamole + mebendazole. Out of the seven combinations screened in the second iteration, six combinations showed varying degrees of synergy within the response matrices (Table 5). Of the newly hypothesized pairs we found three pairs with positive synergy scores: mebendazole + quinacrine, disulfiram + fulvestrant, and disulfiram + quinacrine. The remaining three re-tested combinations also showed consistent positive scores. The three combinations with the highest HSA scores also showed specificity (>1 HSA score) towards MCF7. It is worth mentioning that the most synergistic 3x3 dose response window resulted in one of the combinations (disulfiram + simvastatin) having a synergy score >10. Plots showing HSA synergy graphs for MCF7 and MCF10A derived from Synergyfinder 3.0 can be found in Supplementary Materials Appendix C1 and C2. HSA scores for MCF10A can be found in Table S11.

	Drug1	Drug2	
1	Disulfiram (Alcoholism)	Fulvestrant (Breast cancer)	+
	"Disulfiram exhibited the highest toxicity to MCF7 cells, and both Disulfiram and Fulvestrant preferentially targeted MCF7 over MCF10A. MCF7 is an estrogen-receptor positive cell line, and Fulvestrant is an estrogen receptor antagonist, which degrades the receptor. This combination could target the estrogen-dependent growth of MCF7 cells. Disulfiram's aldehyde dehydrogenase inhibitory action can further increase its toxicity to MCF7 cells."		
2	Mebendazole (Parasitic Infections)	Quinacrine (Malaria/Anti-inflammatory)	+
	"Both Mebendazole and Quinacrine preferentially targeted MCF7 cells. Mebendazole has anti-cancer properties, potentially by disrupting microtubule function. Quinacrine, though primarily an antimalarial, can exert anti-cancer effects, possibly due to its ability to intercalate with DNA and/or inhibit topoisomerase. This combination might have a multi-pronged effect on MCF7 cells, disrupting cellular division and DNA processes."		
3	Disulfiram (Alcoholism)	Mebendazole (Parasitic Infections)	-
	"As Disulfiram demonstrated the highest toxicity to MCF7 cells and Mebendazole also preferentially targeted MCF7, their combination might exert a compounded effect. The combined microtubule disruption by Mebendazole and the aldehyde dehydrogenase inhibition by Disulfiram could cripple the MCF7 cells at multiple fronts."		
4	Disulfiram (Alcoholism)	Quinacrine (Malaria/Anti-inflammatory)	+
	"Disulfiram exhibited the highest toxicity toward MCF7 cells and has been shown to induce oxidative stress and inhibit proteasomal and NF-κB pathways, which are vital for cancer cell survival. Quinacrine, an antimalarial drug, also possesses anti-cancer properties, including the ability to inhibit NF-κB and autophagy, a survival mechanism often upregulated in cancer cells. The combination is expected to potentiate oxidative stress and inhibit survival pathways more effectively in MCF7 cells. Given that both drugs preferentially targeted MCF7 over MCF10A, their combination might enhance selectivity, exploiting their shared mechanisms for a synergistic effect."		

Table 4. GPT4 drug combination recommendations based on results from the first screen. Synergy hypotheses are provided for each of the four combinations.

Drug 1	Drug 2	HSA score	HSA score (max)	Specificity
Disulfiram	Simvastatin	4.75	10.58	2.41
Disulfiram	Fulvestrant	1.81	4.60	0.03
Disulfiram	Quinacrine	1.53	4.47	0.6
Dipyridamole	Mebendazole	1.10	5.26	3.60
Disulfiram	Hydroxychloroquine	1.08	3.06	-1.86
Mebendazole	Quinacrine	0.56	5.54	1.09
Disulfiram	Mebendazole	-2.49	0.13	-1.83

Table 5. Calculated HSA synergy scores for each combination. Two HSA scores are provided, the first considers the entire dose-response matrix, while the second (max) is based on the most synergistic 3-by-3 dose-window in the dose-response matrix. Specificity denotes the difference in the overall HSA synergy score between the two cell lines ($HSA_{MCF7} - HSA_{MCF10A}$) where positive values indicate higher synergy scores for MCF7.

A final query was made to GPT4 requesting future experiments based on the final results (Figure S5). Three drug combinations were recommended: disulfiram + itraconazole, mebendazole + cimetidine, and quinacrine + celecoxib. Hypotheses for these combinations are reported in Table S13. Disulfiram + itraconazole were hypothesized to synergise based on increased oxidative stress and the inhibition of the hedgehog pathway. Mebendazole and cimetidine were also hypothesized to synergise due to their targets being involved in cell cycle progression and growth. The final combination quinacrine + celecoxib had been tested in the initial experiment, suggesting that GPT4 had already “forgotten” its previous recommendations.

It is unclear to what extent GPT4 “understood” its prompt for hypothesis formation. This epistemological uncertainty is shown in the relationship between the explanation of why a pair of drugs would target MCF7 rather than MCF10A (Table S1), and the explanation why MCF10A would not be targeted, where the MCF10A hypotheses are simply negations of the MCF7 ones. More convincing explanations for not targeting MCF10A would have provided us with more confidence in GPT4’s understanding, and the utility of its hypotheses. The hypotheses also exhibited “hallucinations” in their explanations. This is most clearly illustrated by GPT4’s hypothesis that itraconazole would “disrupt(ing) cell membrane integrity”. This explanation presumably originated from the fact that the itraconazole inhibits ergosterol synthesis, which disrupts cell membrane integrity. The factual error is that ergosterol synthesis is not present in mammalian cells. We asked GPT4 “is ergosterol synthesis present in mammalian cells”. It replied “No, ergosterol synthesis is not present in mammalian cells. Ergosterol is a sterol found in the cell membranes of fungi and some protozoa, playing a role similar to cholesterol in mammalian cells...”

We selected cancer treatment as our test domain because every cancer patient ideally requires a scientific research project to understand how best to treat them. In the past this was prohibitively expensive and out of reach for normal cancer patients. The cost of science currently has two main components: the cost of the human scientist’s intelligence, and the laboratory costs. Now, thanks to

the AI revolution, the cost of (machine) scientific intelligence is dropping. Economies of scale could also drive down the cost of the robotics required to automate personalized cancer research. We therefore envision a future where scientific research is cheap enough that every cancer patient can afford treatment based on a personalized research project.

Our empirical results demonstrate that the GPT4 succeeded in its primary task of forming novel and useful hypothesis. We therefore conclude that LLMs are an important source of novel scientific hypotheses for both human scientists and to the increasingly sophisticated AI systems designed to automate science¹¹.

Methods

We employed GPT 4.0 to generate novel drug combinations to treat MCF7 cells, considering criteria such as drug accessibility, FDA approval, and potential synergistic effects. The LLM was prompted to consider information on the mechanism of action such as differential gene expression patterns, pathways, metabolomics, proteomics, lipidomics, genetics, and epigenetics. The prompts can be found in figure S1. Based on the hypotheses generated, we proceeded to experimentally validate thirteen drug combinations, as well as two negative control combinations and two positive control combinations also devised by the LLM.

To avoid drug combinations that have been shown to affect MCF7 in literature, we asked for drug combinations not previously reported and for hypotheses surrounding the choices based on mechanisms of action and synergistic effects. We then attempted to identify any suggested combinations on scholarly databases like PubMed and Google Scholar in an effort to invalidate any suggestions made by GPT4. We have reported our findings with regards to the novelty of combinations in Table 1a, and we could not find any of the combinations reported in MCF7.

As for positive controls, we prompted GPT4 to provide combinations that are currently used in breast cancer treatment and also likely to affect MCF7 (Table 1b). Two combinations, Doxorubicin and Cyclophosphamide, as well as Fulvestrant and Palbociclib were selected. We also prompted negative control combinations, and out of the suggestions we decided to test two combinations, namely Allopurinol and Omeprazole, as well as Diphenhydramine and Cetirizine.

Cell Culture

MCF10A and MCF7 cells were purchased directly from either the American Type Culture Collection (#CRL-10317, ATCC, USA) or the European Collection of Authenticated Cell Lines (#86012803, ECACC, UK), respectively. Cells were cultured in vented tissue culture flasks and incubated at 37°C in a humidified 5% CO₂ atmosphere. Prior to reaching confluence, cells were passaged using TrypLE Select (#12563011, ThermoFisher Scientific, USA), typically every 3–4 days, with a media exchange every 2–3 days. MCF10A cells were cultured in complete MEGM™ Mammary Epithelial Cell Growth Medium BulletKit (#CC-3150, Lonza, Switzerland), supplemented with 100 ng/ml cholera toxin (#C8052-.5MG, Sigma-Aldrich, USA) and 1x Penicillin-Streptomycin (#30-002-CL, Corning, USA). MCF7 cells were cultured in Minimum Essential Medium (MEM) containing Earle's salts and L-glutamine (#10-010-CVR, Corning, USA), supplemented with 10% (v/v) FBS (#10270106, ThermoFisher Scientific, USA), 1x non-

essential amino acids (#11140050, ThermoFisher Scientific, USA) and 1x Penicillin-Streptomycin. For all experiments, cell lines were used at passage \leq +20 (from passage provided by supplier).

Cell Viability Assay

Prior to cell seeding, DMSO-only (negative control) or required compounds (either single agent or combinations) were dispensed in a randomised fashion into white-walled 384w plates (#3765, Corning, USA) at 200x concentration using the D300e Digital Dispenser (TECAN, Switzerland). Wells were normalised to a total volume of 200 nl DMSO (0.5% (v/v) final assay concentration). Following straining through a 100 μ M cell strainer, MCF10a or MCF7 cells were seeded onto compound-containing plates at 5x10³ cells/well in 40 μ l of complete growth medium using the Dragonfly Discovery liquid handler (SPTLabtech, UK), prior to incubation for 48 h at 37°C in a humidified 5% CO₂ atmosphere. 48 h post-compound treatment, cells were equilibrated to 30°C prior to the addition of 40 μ l CellTiter-Glo[®] 3D Cell Viability Assay (#G9682, Promega, USA) reagent using the Dragonfly Discovery liquid handler. Plates were then briefly centrifuge and incubated for 30 min at 30°C in the dark, prior to the acquisition of luminescence signal using a CLARIOstar Plus microplate reader (BMG Labtech, Germany) fitted with a 96/384w aperture spoon (protocol configuration: Ultra-Glo preset, 1s integration time, 3000 gain and 7.5 mm focal height).

Data Analysis

Raw relative luminescence unit (RLU) data was derandomised prior to background subtraction (media only + CellTiter-Glo[®] 3D reagent, no cells) and determination of viability as a percentage of negative control (DMSO only). IC₅₀ values were calculated by applying a four-parameter logistic curve to the response data using AAT bioquest IC₅₀ calculator¹². HSA synergy scores were determined with SynergyFinder 3.0¹³. Four parameter logistic regression (LL4) was used for curve fitting. The correction toggle was enabled for the primary screen where n=1. A HSA synergy score <-10 or >10 is indicative that the interaction between two drugs is likely to be antagonistic or synergistic, respectively. Scores between these values are considered additive.

Primary viability screen

To evaluate the potential synergistic effect of the combinations, we performed a series of cell viability assays using MCF7 cells treated with varying concentrations, individually and in combination. Each experiment was performed once in a primary screen. Dose-response curves were generated to calculate IC₅₀ values where possible, and HSA synergy scores were also calculated, which allowed the determination of whether a drug combination exhibited synergistic, additive, or antagonistic effects. To assess the differential effect of the drug combination on MCF7 and MCF10A cell lines, we performed the same cell viability assays using MCF10A cells. This allowed us to compare the cytotoxic effects of the drug combination on both cell lines and determine the selectivity of the treatment for cancerous cells over non-tumorigenic cells¹⁴. Two-way ANOVA was employed to calculate the significance of a drugs impact on either cell line when compared to the positive control Allopurinol.

Secondary viability screen

Results from the primary screen were summarized and reported back to GPT4. Subsequently, we asked for novel combinations based on these findings using the same set of drugs. See Figure S4 for prompt. We selected four of the novel combinations for validation (mebendazole + quinacrine, disulfiram + mebendazole and disulfiram + fulvestrant, disulfiram + quinacrine). In addition, we validated the results of eleven individual drugs as well as three combinations from the primary screen (disulfiram + simvastatin, disulfiram + hydroxychloroquine and dipyridamole + mebendazole). This second round of experiments were performed using the same assay described above. These experiments ensured sufficient replicates for combinations and single drugs ($n \geq 3$). Due to some outlier readings that significantly altered the mean of the replicates, we chose to use the median value of replicates for our HSA synergy score and IC50 calculations. See prompt in the Sup. Inf.

Data Availability

All experimental data are available in the main text or within the supplement.

References

1. Royal Society. Science in the age of AI: How artificial intelligence is changing the nature and method of scientific research. 978-1-78252-712-1 (2024).
2. Popper, K. The Logic of Scientific Discovery (Hutchinson, London, 1972).
3. Van Veen, D., Van Uden, C., Blankemeier, L., Delbrouk, J-B., Aali, A. et al. Adapted large language models can outperform medical experts in clinical text summarization. *Nat Med* 30, 1134–1142 (2024).
4. Liu, P.J., Saleh, M., Pot, E., Goodrich, B., Sepassi, R., Kaiser, L. & Shazeer, N. Generating Wikipedia by summarizing long sequences. *arXiv preprint arXiv:1801.10198* (2018).
5. Devlin J., Chang, M-W., Lee, K. & Toutanova, K. BERT: Pre-training of Deep Bidirectional Transformers for Language Understanding. *ArXiv Computation and Language. arXiv:1810.04805 [cs.CL]* (2018).
6. Chen, M., Tworek, J., Jun, H., Yuan, Q., Pinto, H. et al. Evaluating large language models trained on code, *arXiv:2107.03374 [cs.LG]* (2021).
7. Zhang, B., Reklou, I., Jain, N., Peñuela, A.M. & Simperl, E., Using Large Language Models for Knowledge Engineering (LLMKE): A Case Study on Wikidata. *arXiv preprint arXiv:2309.08491* (2023).
8. Radford, A., Wu, J., Child, R., Luan, D., Amodei, D. & Sutskever, I., et al. Language models are unsupervised multitask learners. *Technical Report, OpenAI blog*, 1 (8): 9 (2019).
9. Sourati, J. & Evans, J.A. Accelerating science with human-aware artificial intelligence. *Nat Hum Behav* 7, 1682–1696 (2023).
10. Zenil, H., Tegner, J., Abrahao., F.S., Lavin, A., Kumar, V. et al. The Future of Fundamental Science Led by Generative Closed-Loop Artificial Intelligence, *arXiv:2307.07522v3 [cs.AI]* (2023).
11. King, R. D., Rowland, J., Oliver, S. G., Young, M., Aubrey, W. et. al. The automation of science. *Science (New York, N.Y.)*, 324(5923), 85–89 (2009).
12. AAT Bioquest, Inc., December 18). Quest Graph™ IC50 Calculator. AAT Bioquest. <https://www.aatbio.com/tools/ic50-calculator> (2023).

13. Ianevski, A., Giri, K. A. & Aittokallio, T. "SynergyFinder 3.0: an interactive analysis and consensus interpretation of multi-drug synergies across multiple samples." *Nucleic Acids Research* 50(W1):W739-W743 (2022).
14. Debnath, J., Muthuswamy, S.K. & Brugge, J.S. Morphogenesis and oncogenesis of MCF-10A mammary epithelial acini grown in three-dimensional basement membrane cultures. *Methods*. 30(3):256-68 (2003).